Rosengarth A, Gerke V, Luecke H. 2001. X-ray structure of full-length annexin 1 and implications for membrane aggregation. J Mol Biol 306: 489–498.

Scheffner M, Staub O. 2007. HECT E3s and human disease. BMC Biochem 8 (Suppl 1): S6.

Scheffner M, Huibregtse JM, Vierstra RD, Howley PM. 1993. The HPV-16 E6 and E6-AP complex functions as a ubiquitin-protein ligase in the ubiquitination of p53. Cell 75:495–505.

Scheffner M, Huibregtse JM, Howley PM. 1994. Identification of a human ubiquitin-conjugating enzyme that mediates the E6-AP-dependent ubiquitination of p53. Proc Natl Acad Sci USA 91:8797–8801.

Shirakura M, Murakami K, Ichimura T, Suzuki R, Shimoji T, Fukuda K, Abe K, Sato S, Fukasawa M, Yamakawa Y, Nishijima M, Moriishi K, Matsuura Y, Wakita T, Suzuki T, Howley PM, Miyamura T, Shoji I. 2007. E6AP ubiquitin ligase mediates ubiquitylation and degradation of hepatitis C virus core protein. J Virol 81:1174–1185.

Skouteris GG, Schroder CH. 1996. The hepatocyte growth factor receptor kinase-mediated phosphorylation of lipocortin-1 transduces the proliferating signal of the hepatocyte growth factor. J Biol Chem 271:27266–27273.

Solito E, Christian HC, Festa M, Mulla A, Tierney T, Flower RJ, Buckingham JC. 2006. Post-translational modification plays an essential role in the translocation of annexin A1 from the cytoplasm to the cell surface. FASEB J 20:1498–1500.

Staub O, Dho S, Henry P, Correa J, Ishikawa T, McGlade J, Rotin D. 1996. WW domains of Nedd4 bind to the proline-rich PY motifs in the epithelial Na+ channel deleted in Liddle's syndrome. EMBO J 15:2371–2380.

Talis AL, Huibregtse JM, Howley PM. 1998. The role of E6AP in the regulation of p53 protein levels in human papillomavirus (HPV)-positive and HPV-negative cells. J Biol Chem 273:6439–6445.

Varticovski L, Chahwala SB, Whitman M, Cantley L, Schindler D, Chow EP, Sinclair LK, Pepinsky RB. 1988. Location of sites in human lipocortin I that are phosphorylated by protein tyrosine kinases and protein kinases A and C. Biochemistry 27:3682–3690.

Yang Y, Liu W, Zou W, Wang H, Zong H, Jiang J, Wang Y, Gu J. 2007. Ubiquitin-dependent proteolysis of trihydrophobin 1 (TH1) by the human papilloma virus E6-associated protein (E6-AP). J Cell Biochem 101:167–180.

Original Article

Intervirology

Intervirology 2010;53:49–54
DOI: 10.1159/000252784

Published online: January 5, 2010

Outcome and Early Viral Dynamics with Viral Mutation in PEG-IFN/RBV Therapy for Chronic Hepatitis in Patients with High Viral Loads of Serum HCV RNA Genotype 1b

Noriko Sasase[a] Soo Ryang Kim[b] Masatoshi Kudo[e] Ke Ih Kim[a]
Miyuki Taniguchi[b] Susumu Imoto[b] Keiji Mita[b] Yoshitake Hayashi[c]
Ikuo Shoji[d] Ahmed El-Shamy[d] Hak Hotta[d]

Departments of [a]Pharmacy and [b]Gastroenterology, Kobe Asahi Hospital, [c]Center for Infectious Diseases and [d]Division of Microbiology, Kobe University Graduate School of Medicine, Kobe, and [e]Department of Gastroenterology and Hepatology, Kinki University School of Medicine, Osaka-Sayama, Japan

Key Words
Chronic hepatitis · Early viral dynamics · IFN/RBV resistance-determining region · HCV RNA genotype 1b · High viral load · PEG-IFN/RBV combination therapy · Virological response, prediction

Abstract
We investigated whether sustained virological response (SVR) and non-SVR by chronic hepatitis C patients to pegylated interferon plus ribavirin (PEG-IFN/RBV) combination therapy are distinguishable by viral factors such as the IFN/RBV resistance-determining region (IRRDR) and by on-treatment factors through new indices such as the rebound index (RI). The first RI (RI-1st; the viral load at week 1 divided by the viral load at 24 h) and the second RI (RI-2nd; the viral load at week 2 divided by the viral load at 24 h) were calculated. The subject patients were divided into 3 groups based on RI-1st and RI-2nd: an RI-A group (RI-1st ≤1.0), an RI-B group (RI-1st >1.0 and RI-2nd <0.7) and an RI-C group (RI-1st >1.0 and RI-2nd ≥0.7). The SVR rate was 71.4% (10/14) in the RI-A group, 46.2% (6/13) in the RI-B group and 20.0% (3/15) in the RI-C group ($p = 0.005$ between the RI-A group and the RI-C group). In IRRDR ≥6 and IRRDR ≤5 the SVR rate was 81.3% (13/16) and 23.1% (6/26) ($p = 0.0002$), respectively. By combining RI and IRRDR as a predicting factor, the SVR rate was 87.5% (7/8) in the RI-A group (≥6 mutations in the IRRDR) and 7.7% (1/13) in the RI-C group (≤5 IRRDR mutations) ($p = 0.0003$).

Introduction

Recently, global consensus has obtained that a combination of IFN or pegylated IFN plus ribavirin (PEG-IFN/RBV) is the treatment of choice for chronic hepatitis C (CHC). Notwithstanding this treatment regimen, sustained virological response (SVR) rates of those infected with the most resistant genotypes [hepatitis C virus (HCV)-1a and -1b] still hover at ~50% [1, 2]. It is therefore worthwhile to identify the predictive factors that allow the selection of patients who would achieve eradication

KARGER
Fax +41 61 306 12 34
E-Mail karger@karger.ch
www.karger.com

0300–5526/10/0531–0049$26.00/0

Accessible online at:
www.karger.com/int

Soo Ryang Kim, MD
Department of Gastroenterology
Kobe Asahi Hospital
3-5-25 Bououji-cho, Nagata-ku, Kobe 653-0801 (Japan)
Tel. +81 78 612 5151, Fax +81 78 612 5152, E-Mail asahi-hp@arion.ocn.ne.jp

of HCV RNA either before or during therapy, especially since IFN/RBV combination therapy is costly and has several side effects [3].

Predictors of the effectiveness of IFN-based therapy can be classified into pretreatment and on-treatment factors. Pretreatment factors comprise: (1) host factors such as age, gender, obesity, alcohol consumption, hepatic iron overload, fibrosis, immune responses and co-infection with other viruses, and (2) viral factors that mainly include viral genotypes and loads, particular amino acid sequence variations in the NS5A region [4, 5] and in the core protein region of HCV [6] within a given genotype. Moreover, the mean number of mutations in variable region 3 (V3) plus its upstream flanking region of NS5A [amino acid 2334–2379, referred to as IFN/RBV resistance-determining region (IRRDR)] is significantly higher in HCV isolates obtained from patients who later achieve SVR by PEG-IFN/RBV than in those from non-SVR patients. On-treatment factors are mainly related to viral kinetics within the first few weeks of treatment [7].

In the current study, with the aim of investigating whether SVR and non-SVR can be distinguished by viral factors such as IRRDR and by on-treatment factors through new indices such as the rebound index (RI), we calculated the first RI (RI-1st; the viral load at week 1 divided by the viral load at 24 h) and the second RI (RI-2nd; the viral load at week 2 divided by the viral load at 24 h), as proposed by Nomura et al. [8].

Patients and Methods

The 42 patients included in this study, who all demonstrated high viral loads (>100 KIU/ml) of serum HCV RNA of genotype 1b, had been diagnosed with CHC on the basis of abnormal serum alanine aminotransferase persisting for at least 6 months, and of positive HCV RNA assessed by RT-PCR. None of the patients was positive for hepatitis B surface antigen or other liver diseases (autoimmune hepatitis, alcoholic liver disease). All the patients received a regimen of PEG-IFNα-2b (peginterferon alpha-2b; PegIntron; Schering-Plough, Kenilworth, N.J., USA) (1.5 μg/kg/week, subcutaneously) in combination with RBV (ribavirin; Rebetol; Schering-Plough) 600–1,000 mg/day for 48 weeks. RBV was administered at a dose of 600 mg/day (3 capsules) to patients weighing <60 kg, 800 mg/day (4 capsules) to those weighing <80 kg and 1,000 mg/day (5 capsules) to those weighing ≥80 kg.

The efficacy of the combination therapy was evaluated by HCV RNA negativity determined by qualitative RT-PCR analysis at the end of therapy (end of therapy response) and 6 months after the completion of therapy (SVR). The amount of HCV RNA was also measured quantitatively by RT-PCR (Amplicor HCV monitor v. 2.0; Roche) before therapy. The lower detection limit of the assay was 5 KIU/ml. Samples collected during and after therapy were also determined by qualitative RT-PCR (Amplicor; Roche), which has a higher sensitivity than quantitative analysis, and the results were labeled as positive or negative. The lower limit of the assay was 50 IU/ml.

SVR was defined as undetectable serum HCV RNA at 24 weeks after the cessation of treatment, and non-SVR as detectable HCV RNA at 24 weeks after the discontinuation of treatment. Informed consent was obtained from all patients enrolled in the study after thoroughly explaining the aims, risks and benefits of the therapy.

The amount of HCV core antigen was assessed by the IRM assay (Ortho Clinical Diagnostics, Tokyo, Japan), which provides a good correlation between the amount of HCV core antigen and the amount of HCV RNA, as shown in our previous study [9]. The HCV core antigen was measured on days 0, 1 (24 h), 7 (1 week) and 14 (2 weeks) according to the detection limit of 20 fmol/l established by the manufacturer.

RI-1st was defined as the coefficient derived by dividing the viral load of HCV core antigen at week 1 by that at 24 h, and RI-2nd was defined as the coefficient derived by dividing the viral load at week 2 by that at 24 h [8].

The patients were divided into 3 groups based on RI-1st and RI-2nd: group A (RI-1st ≤1.0), group B (RI-1st >1.0 and RI-2nd <0.7) and group C (RI-1st >1.0 and RI-2nd ≥0.7).

NS5A sequence analysis (IRRDR) was performed as described [4]. Briefly, the sequences of the amplified fragments were determined by direct sequencing without subcloning with the use of a Big Dye Deoxy Terminator cycle sequencing kit and an ABI 337 DNA sequencer (Applied Biosystems, Japan). The aa sequences were deduced and aligned with Genetyx Win software v. 7.0 (Genetyx Corp., Tokyo, Japan). Numbering of aa throughout the manuscript is according to the polyprotein of HCV genotype 1b prototype HCV-J.

Statistical Analysis

Differences between the groups were assessed by the χ^2 test, Fisher's exact test or Student's t test, the Mann-Whitney test and the Kruskal-Wallis test. $p < 0.05$ was considered statistically significant.

Results

Of the 42 patients treated with combination therapy, 19 (45.2%) achieved SVR and 23 (54.8%) were still HCV RNA positive (non-SVR) 6 months after therapy. No significant differences were observed in patient characteristics between SVR and non-SVR, except in platelet counts and the degree of fibrosis (table 1), or among the RI-A, -B and -C groups (table 2).

The SVR rate was 71.4% (10/14), 46.2% (6/13) and 20.0% (3/15) in the RI-A, -B and -C groups, respectively, with a significant difference between the RI-A and -C groups ($p = 0.005$), but not significant between the RI-A and -B groups and the RI-B and -C groups (fig. 1). In the 14 patients of the RI-A group, HCV RNA turned negative

Table 1. Host-dependent, virus-related profile by response (SVR and non-SVR)

	SVR	Non-SVR	p value
Gender (M/F), n	11/8	13/10	NS
Age, years	56.7 ± 8.8	59.3 ± 10.5	NS
HCV RNA level, KIU/ml	1,685 ± 1,477	1,660 ± 1,363	NS
HCV core antigen, fmol/l	7,044 ± 6,763	9,343 ± 12,563	NS
Body weight, kg	59.9 ± 11.5	59.8 ± 13.6	NS
Treatment history (retreatment/naïve)	6/13	13/10	NS
Platelet count ($\times 10^4$/mm^3)	18.7 ± 4.4	14.8 ± 5.4	0.02
F0, 1/F2, 3	12/2	5/10	0.004

Table 2. Host-dependent, virus-related profile by response (RI-A, -B and -C groups)

	RI-A	RI-B	RI-C	p value
Gender (M/F), n	7/7	9/4	8/7	NS
Age, years	60.0 ± 5.9	58.5 ± 9.4	56.1 ± 12.8	NS
HCV RNA level, KIU/ml	1,401 ± 1,014	2,053 ± 1,286	1,593 ± 1,772	NS
HCV core antigen, fmol/l	6,084 ± 5,106	7,674 ± 5,038	11,000 ± 15,837	NS
Body weight, kg	62.1 ± 16.6	59.5 ± 10.4	58.2 ± 10.1	NS
Treatment history (retreatment/naïve)	3/11	7/6	9/6	NS
Platelet count ($\times 10^4$/mm^3)	15.3 ± 3.5	18.3 ± 5.9	16.3 ± 6.0	NS
F0, 1/F2, 3	7/3	5/4	5/5	NS

Table 3. SVR rate between IRRDR ≤5 and IRRDR ≤6 in RI-A, -B and -C groups

	RI-A		RI-B		RI-C	
	IRRDR ≤5	IRRDR ≥6	IRRDR ≤5	IRRDR ≥6	IRRDR ≤5	IRRDR ≥6
SVR	3	7	2	4	1	2
Non-SVR	3	1	5	2	12	0
SVR rate, %	50.0	87.5	28.6	66.7	7.7	100
p value	NS		NS		0.0024	
	0.0003					

by week 4 in 3 patients, week 8 in 5 patients, week 12 in 5 patients and was positive in 1 patient throughout the treatment. In the 13 patients of the RI-B group, HCV RNA was negative by week 4 in 1 patient, week 8 in 2 patients, week 12 in 4 patients, at and after week 16 in 5 patients and remained positive throughout the treatment in 1 patient. In the 15 patients of the RI-C group, HCV RNA was negative by week 12 in 1 patient, on and after week 16 in 6 patients and remained positive throughout the treatment in 8 patients (fig. 2).

The SVR rate was 81.3% (13/16) in the group with ≥6 mutations in IRRDR, and 23.1% (6/26) in those with ≤5 (fig. 3), with a significant difference between the 2 groups (p = 0.0002).

By combining RI and IRRDR, the SVR rate was 87.5% (7/8) in the RI-A group (IRRDR ≥6) and 7.7% (1/13) in the RI-C group (IRRDR ≤5) (table 3), with a significant difference between the 2 groups (p = 0.0003).

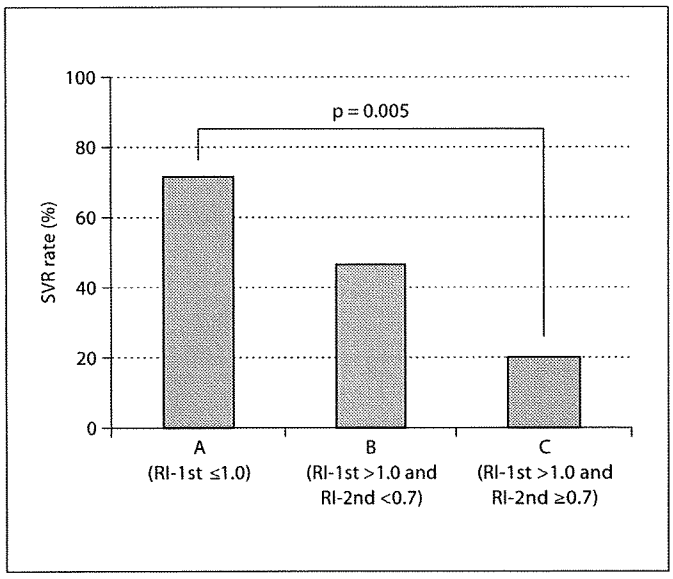

Fig. 1. SVR rate in RI-A, -B and -C groups. The overall SVR rate was 71.4, 46.2 and 20.0%, respectively. Significant difference in SVR rate is indicated.

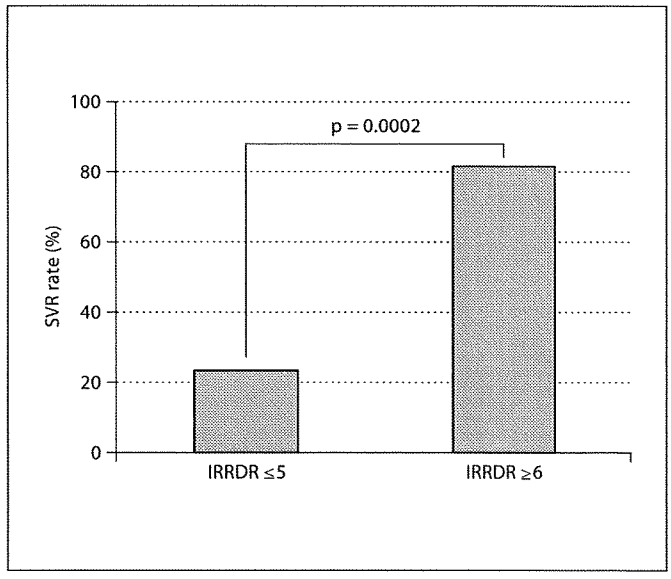

Fig. 3. SVR rate and IRRDR number. The SVR rate was 23.1% in IRRDR ≤5 and 81.3% in IRRDR ≥6, which was significantly different.

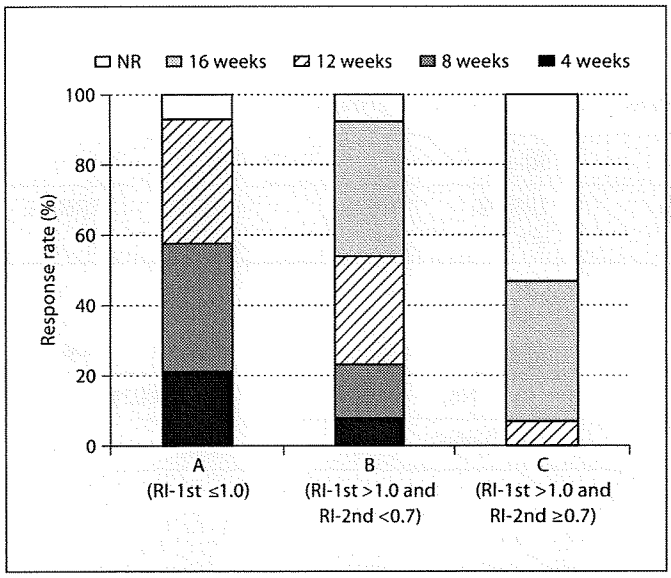

Fig. 2. Relation between response time and virus dynamics. In the 14 patients of the RI-A group, HCV RNA turned negative by week 4 in 3 patients, week 8 in 5 patients, week 12 in 5 patients and remained positive throughout the treatment in 1 patient. In the 13 patients of the RI-B group, HCV RNA was negative by week 4 in 1 patient, week 8 in 2 patients, week 12 in 4 patients, at and after week 16 in 5 patients and remained positive throughout the treatment in 1 patient. In the 15 patients of the RI-C group, HCV RNA was negative by week 12 in 1 patient, at and after week 16 in 6 patients and remained positive throughout the treatment in 8 patients.

Discussion

The importance of early virological response (EVR; signifying HCV RNA negative at 12 weeks) has been emphasized in predicting SVR and non-SVR in CHC patients undergoing IFN treatment; those not reaching EVR do not respond to further therapy. Discontinuation of treatment in patients not reaching EVR would reduce drug costs by more than 20%; consequently, early confirmation of viral reduction after initiating antiviral therapy for CHC is worth investigating [10].

Treatment with IFN induces a decline in HCV RNA levels that can be mathematically measured in 2 phases. The decline in the first phase, usually measured at 24 or 48 h, probably reflects direct inhibition of intracellular production and release of HCV [11], with IFN efficacy ranging from about 70% (approx. 0.7 log units) for standard IFN (given 3 times a week) to more than 90% (1 log unit) for high daily doses of standard IFN or PEG-IFN (given once a week) [12, 13]. The decline in the second phase, beginning after 24–48 h, is slower and more variable than that in the first phase, and is thought to reflect continued inhibition of replication and the gradual elimination of virus-infected cells [11]. The decay in the first phase has little correlation with the IFN dose, but is more rapid with PEG-IFN than with standard IFN preparations [10].

Lowering HCV RNA during the first phase is essential for efficient elimination of HCV during the second phase. Decreases in HCV RNA titers within the first 24–48 h after the start of IFN would, therefore, be a dependable estimate of antiviral efficacy [12, 13].

Early viral kinetics, determined up to week 2, are believed to express the therapeutic effect of PEG-IFN. The concentration of PEG-IFNα-2b in serum peaks after 24 h, then declines gradually [14, 15]. The viral load is thus reduced by 24 h but increases in week 1 [16, 17]; with a large dose of PEG-IFN at each administration, it decreases markedly at 24 h but then increases in week 1 regardless of the dose. In the responder group, however, the viral load continues to decline each week thereafter [17].

In this study, we used new indices proposed by Nomura et al. [8]: RI-1st and RI-2nd calculated from early viral kinetics. RI-1st was defined as the coefficient derived by dividing the viral load of HCV core antigen at week 1 by that at 24 h, and the RI-2nd was defined as the coefficient derived by dividing the viral load at week 2 by that at 24 h. In the SVR group, a number of patients demonstrated no increase in the viral load at week 1. Patients with a high RI-2nd were regarded as poor responders or non-responders to PEG-IFN. The RI-2nd of those other than non-responders was below 0.7; therefore, 0.7 was adopted as the reference value for RI-2nd, and the patients were divided into 3 groups based on RI-1st and RI-2nd: the RI-A group (RI-1st $\leq$1.0), the RI-B group (RI-1st >1.0 and RI-2nd <0.7) and the RI-C group (RI-1st >1.0 and RI-2nd $\geq$0.7). The SVR rate of the RI-A, RI-B and RI-C groups was 71.4% (10/14), 46.2% (6/13) and 20% (2/10), respectively (p = 0.005 between the RI-A group and the RI-C group). RIs are also associated with the early clearance of HCV RNA that is related to SVR.

In the RI-A group 21.4% (3/14), 35.7% (5/14) and 35.7% (5/14) became HCV RNA negative by weeks 4, 8 and 12, respectively. In the RI-B group 7.7% (1/13), 15.4% (2/13), 30.8% (4/13) and 38.5% (5/13) became HCV RNA negative by weeks 4, 8, 12, and at and after week 16, respectively. In the RI-C group 6.7% (1/15) and 40.0% (6/15) became HCV RNA negative by week 12, and at and after week 16, respectively. It is believed that the simplified RI-1st and RI-2nd are evidential indices for determining the therapeutic efficacy of PEG-IFN/RBV treatment.

We have previously reported that the high degree of sequence variation in IRRDR (IRRDR $\geq$6) significantly correlates with SVR, whereas the low degree of sequence variation in this region (IRRDR $\leq$5) correlates with non-SVR [4]. A significant correlation between the rapid reduction of HCV core antigen titers and the degree of sequence variation in IRRDR has been observed. This, in particular, suggests a possible influence of IRRDR $\geq$6 on HCV replication kinetics during IFN-based therapy, especially that the direct effect of IFN begins a few hours after the first dose.

In this study, the SVR rate was 81.2% (13/16) with IRRDR $\geq$6 and 23.1% (6/26) with IRRDR $\leq$5 (p = 0.0002), strongly suggesting that IRRDR $\geq$6 would be a useful marker for the prediction of SVR.

By combining RI and IRRDR as a predicting factor, the SVR rate was 87.5% (7/8) in the RI-A group (RI-1st $\leq$1.0) with IRRDR $\geq$6, signifying that about 90% of these patients turned SVR and were, thus, believed to be very good responders. An SVR rate of 7.7% (1/13) was obtained in the RI-C group with IRRDR $\leq$5 (p = 0.0003).

In conclusion, we propose that IRRDR combined with RIs is the most sensitive predictive factor for SVR and non-SVR. With the aid of RIs and IRRDR, a more effective PEG-IFN/RBV treatment could be within reach. A more detailed investigation with a larger number of subjects is needed to confirm the current results in patients given PEG-IFN/RBV combination therapy.

Acknowledgment

We are indebted to Yoshiko Kawamura for assistance in the preparation of the manuscript.

Disclosure Statement

No conflict of interest exists.

References

1 Manns MP, McHutchison JG, Gordon SC, Rustgi VK, Shiffman M, Reindollar R, et al: Peginterferon alfa-2b plus ribavirin compared with interferon alfa-2b plus ribavirin for initial treatment of chronic hepatitis C: a randomised trial. Lancet 2001;358:958–965.

2 Fried MW, Shiffman ML, Reddy KR, Smith C, Marinos G, Goncales FL Jr, et al: Peginterferon alfa-2a plus ribavirin for chronic hepatitis C virus infection. N Engl J Med 2002; 347:975–982.

3 Nakamura H: Early prediction of sustained viral responder and non-responder during interferon and ribavirin combination therapy in chronic hepatitis C. Hepatol Res 2005; 33:269–271.

4 El-Shamy A, Nagano-Fujii M, Sasase N, Imoto S, Kim SR, Hotta H: Sequence variation in hepatitis C virus nonstructural protein 5A predicts clinical outcome of pegylated interferon/ribavirin combination therapy. Hepatology 2008;48:38–47.
5 Enomoto N, Sakuma I, Asahina Y, Kurosaki M, Murakami T, Yamamoto C, Ogura Y, Izumi N, Marumo F, Sato C: Mutations in the nonstructural protein 5A gene and response to interferon in patients with chronic hepatitis C virus 1b infection. N Engl J Med 1996; 334:77–81.
6 Akuta N, Suzuki S, Kawamura Y, Yatsuji H, Sezaki H, Suzuki Y, Hosaka T, Kobayashi M, Kobayashi M, Arase Y, Ikeda K, Miyakawa Y, Kumada H: Prediction of response to pegylated interferon and ribavirin in hepatitis C by polymorphism in the viral core protein and very early dynamics of viremia. Intervirology 2007;50:361–368.
7 Ferenci P: Predictors of response to therapy for chronic hepatitis C. Semin Liver Dis. 2004;24:S25–S31.
8 Nomura H, Miyagi Y, Tanimoto H, Higashi M, Ishibashi H: Effective prediction of outcome of combination therapy with pegylated interferon alpha 2b plus ribavirin in Japanese patients with genotype-1 chronic hepatitis C using early viral kinetics and new indices. J Gastroenterol 2009;44:338–345.
9 Sasase N, Kim SR, Kim KI, Taniguchi M, Imoto S, Hotta H, Shouji I, El-Shamy A, Kawada N, Kudo M, Hayashi Y: Usefulness of a new immunoradiometric assay of HCV core antigen to predict virological response during PEG-IFN/RBV combination therapy for chronic hepatitis with high viral load of serum HCV RNA genotype 1b. Intervirology 2008;51:S70–S75.
10 Davis GL: Monitoring of viral levels during therapy of hepatitis C. Hepatology 2002;36: S145–S151.
11 Neumann AU, Lam NP, Dahari H, Gretch DR, Wiley TE, Layden TJ, Perelson AS: Hepatitis C viral dynamics in vivo and the antiviral efficacy of interferon-α therapy. Science 1998;282:103–107.
12 Lam NP, Neumann AU, Gretch DR, Wiley TE, Perelson AS, Layden TJ: Dose-dependent acute clearance of hepatitis C genotype 1 virus with interferon alfa. Hepatology 1997;26:226–231.
13 Zeuzem S, Herrmann E, Lee JH, Fricke J, Neumann AU, Modi M, Colucci G, Roth WK: Viral kinetics in patients with chronic hepatitis C treated with standard or peginterferon alfa-2a. Gastroenterology 2001;120: 1438–1447.
14 Silva M, Poo J, Wagner F, Jackson M, Cutler D, Grace M, et al: A randomized trial to compare the pharmacokinetic, pharmacodynamic, and antiviral effects of peginterferon alfa-2b and peginterferon alfa-2a in patients with chronic hepatitis C (COMPARE). J Hepatol 2006;45:204–213.
15 Asahina Y, Izumi N, Umeda N, Hosokawa T, Ueda K, Doi F, et al: Pharmacokinetics and enhanced PKR response in patients with chronic hepatitis C treated with pegylated interferon alpha-2b and ribavirin. J Viral Hepat 2007;14:396–403.
16 Izumi N, Asahina Y, Kurosaki M, Uchihara M, Nishimura Y, Inoue K, et al: A comparison of the exponential decay slope between PEG-IFN alfa-2b/ribavirin and IFN alfa-2b/ribavirin combination therapy in patients with chronic hepatitis C genotype 1b infection and a high viral load. Intervirology 2004;47:102–107.
17 Buti M, Sanchez-Avila F, Lurie Y, Stalgis C, Valdes A, Martell M, et al: Viral kinetics in genotype 1 chronic hepatitis C patients during therapy with 2 different doses of peginterferon alfa-2b plus ribavirin. Hepatology 2002;35:930–936.

Oncogene (2009) 28, 469–478

www.nature.com/onc

ORIGINAL ARTICLE

A novel mouse model of hepatocarcinogenesis triggered by AID causing deleterious p53 mutations

A Takai[1], T Toyoshima[3], M Uemura[3], Y Kitawaki[2], H Marusawa[1], H Hiai[3], S Yamada[4], IM Okazaki[2], T Honjo[2], T Chiba[1] and K Kinoshita[3]

[1]Department of Gastroenterology and Hepatology, Graduate School of Medicine, Kyoto University, Kyoto, Japan; [2]Department of Immunology and Genomic Medicine, Graduate School of Medicine, Kyoto University, Kyoto, Japan; [3]Shiga Medical Center Research Institute, Moriyama, Japan and [4]Mikasa Laboratory, Immuno-Biological Laboratories Co., Ltd, Mikasa, Japan

Activation-induced cytidine deaminase (AID), the only enzyme that is known to be able to induce mutations in the human genome, is required for somatic hypermutation and class-switch recombination in B lymphocytes. Recently, we showed that AID is implicated in the pathogenesis of human cancers including hepatitis C virus (HCV)-induced human hepatocellular carcinoma (HCC). In this study, we established a new AID transgenic mouse model (TNAP-AID) in which AID is expressed in cells producing tissue-nonspecific alkaline phosphatase (TNAP), which is a marker of primordial germ cells and immature stem cells, including ES cells. High expression of TNAP was found in the liver of the embryos and adults of TNAP-AID mice. HCC developed in 27% of these mice at the age of approximately 90 weeks. The HCC that developed in TNAP-AID mice expressed α-fetoprotein and had deleterious mutations in the tumour suppressor gene *Trp53*, some of which corresponded to those found in human cancer. In conclusion, TNAP-AID is a mouse model that spontaneously develops HCC, sharing genetic and phenotypic features with human HCC, which develops in the inflamed liver as a result of the accumulation of genetic changes.
Oncogene (2009) **28**, 469–478; doi:10.1038/onc.2008.415; published online 10 November 2008

Keywords: hepatic cancer; stem cell marker; activation-induced cytidine deaminase; Cre recombinase; somatic mutation; animal model

Introduction

It is widely recognized that mutations of oncogenes, tumour suppressor genes and genomic stability genes play pivotal roles in cancer development (Vogelstein and Kinzler, 2004). Despite remarkable progress in our knowledge of the molecular mechanisms of individual cancer-related genes, surprisingly little is known about the fundamental aspects of when and how mutations are introduced into what kind of cell populations (for example, differentiated cells versus tissue stem cells).

To address this problem, a new mechanism of mutagenesis for cancer development has recently been proposed (Kinoshita and Nonaka, 2006; Marusawa, 2008). It hypothesizes that at least some cancer-related mutations are introduced by activation-induced cytidine deaminase (AID), an enzyme that is expressed in activated B lymphocytes, and is required for somatic hypermutation (SHM) and class-switch recombination of antibody genes (Honjo *et al.*, 2002). The hypothesis is based on the following observations: (1) AID can induce mutations in non-B cells (Yoshikawa *et al.*, 2002); (2) AID transgenic mice develop various tumours, including T-cell lymphoma and lung microadenoma (Okazaki *et al.*, 2003) and (3) AID can be induced in human hepatic, gastric and biliary epithelial cells when stimulated with pro-inflammatory cytokines, such as transforming growth factor-β and tumor necrosis factor-α, and when challenged with pathogens, such as hepatitis C virus (HCV) and *Helicobacter pylori*. AID is detected in the liver, stomach and bile duct in humans (Kou *et al.*, 2006; Endo *et al.*, 2007; Matsumoto *et al.*, 2007; Komori *et al.*, 2008). On the basis of this evidence, AID is a potential candidate for a mutagen in human cancers.

To substantiate this hypothesis, there is an urgent need for the establishment of an AID transgenic mouse model that recapitulates the development of human cancer. However, we have found earlier that it is difficult to analyse epithelial tumours of tissues other than lymphoid malignancies in a transgenic mouse model with constitutive and ubiquitous AID expression because of early death of the mice from lethal T-cell lymphoma (Okazaki *et al.*, 2003).

We generated earlier AID transgenic mice that can express AID conditionally in a Cre-recombianase-dependent manner (AID conditional transgenic, AID cTg) and reported B-cell-specific AID transgenic mice

Correspondence: Dr K Kinoshita, Evolutionary Medicine, Shiga Medical Center Research Institute, 5/4/1930, Moriyama, Shiga 524-8524, Japan.
E-mail: kkinoshi.shigamed@mac.com
Received 30 June 2008; revised 30 September 2008; accepted 14 October 2008; published online 10 November 2008

obtained by crossing AID cTg mice with B-cell-specific Cre transgenic mice (Muto *et al.*, 2006). In this study, we used a different Cre transgenic mouse line that expresses Cre in cells producing tissue nonspecific alkaline phosphatase (TNAP), as the mating partner of AID cTg mice.

TNAP is a member of the alkaline phosphatase family encoded by the *Akp2* gene and alternatively designated alkaline phosphatase 2, liver. As TNAP is also known as a marker of primordial germ cells and immature stem cells, including ES cells (Urven *et al.*, 1993; Kues *et al.*, 2005; Wang *et al.*, 2005), we initially speculated that AID expression in TNAP-positive cells might contribute to the development of tumours of germ cell origin. However, the resulting mice frequently developed hepatocellular carcinoma (HCC) but not germ cell tumours or lethal lymphomas. Histological and molecular analyses of HCC revealed genetic and phenotypic similarities to human tumours, including deleterious mutations in the p53 gene and the expression of α-fetoprotein, a well-known marker of human HCC. This mouse model should be useful for studies on the prevention and treatment of hepatic cancer, which is a major health concern worldwide.

Results

We crossed AID cTg mice with TNAP-Cre mice (Lomeli *et al.*, 2000; Figures 1a and b). AID cTg mice possess a CAG promoter-driven AID transgene, whose expression is blocked by insertion of the gene encoding enhanced green fluorescent protein (hereafter GFP) flanked by two loxP sites (Figure 1a). Therefore, the expression of Cre recombinase removes GFP and induces AID expression (Muto *et al.*, 2006). TNAP-Cre mice were generated by inserting the coding sequence of Cre recombinase into the *Akp2* locus of the 129/Sv mouse genome, and Cre was expressed in primordial germ cells in the embryonic genital ridge region (Lomeli *et al.*, 2000). We crossed homozygous female AID cTg mice on a C57BL/6 background with heterozygous male TNAP-Cre mice to obtain double-transgenic mice (TNAP-AID) and their littermate control AID cTg mice. Non-transgenic (wild-type, WT) and TNAP-Cre control mice on a C57BL/6:129/Sv hybrid background were obtained by mating female C57BL/6 mice with heterozygous male TNAP-Cre mice (Figure 1b). Accordingly, a total of 101 mice were prepared, which included 28 TNAP-AID, 29 AID cTg, 16 TNAP and 28 WT mice.

Most mice were viable at 90 weeks (Figure 1c), whereas in our earlier study, most AID transgenic mice died because of the lethal lymphoid malignancies, majority of which died within 50 weeks (Okazaki *et al.*, 2003). Although TNAP is expressed in primordial germ cells, we did not observe any incidence of testicular or ovarian tumours in TNAP-AID mice. Instead of germ cell tumours, we frequently observed macroscopic liver tumours in TNAP-AID mice. Table 1 summarizes

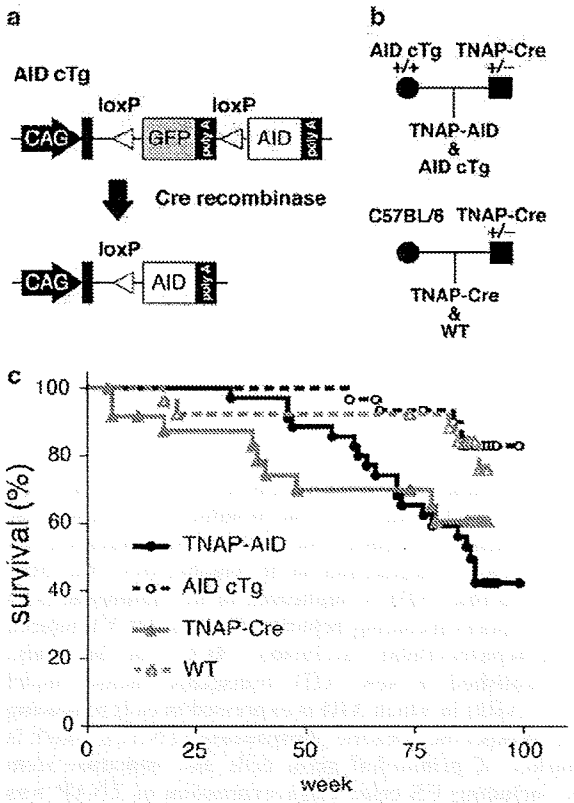

Figure 1 Generation of TNAP-AID mice and their controls. (**a**) Structure of transgene used to generate AID conditional transgenic mice (AID cTg) and the structure after Cre-mediated recombination. Arrows indicate the CAG promoter and rectangles indicate exons. Grey and open boxes represent the coding sequences of GFP and AID, respectively. A polyadenylation signal (poly A) is attached after each coding sequence. Triangles indicate loxP sites. (**b**) Mating scheme. For genotype abbreviations, see text. (**c**) Kaplan–Meier survival curves for the four genotype groups.

the frequency and spectrum of tumours that developed in TNAP-AID and control mice. Interestingly, liver tumours were observed in TNAP-AID mice but not in the control groups; the difference between TNAP-AID and AID cTg mice ($P = 0.017$) and that between TNAP-AID and WT mice ($P = 0.018$) was significant. There were no differences among the groups with regard to weights of body, liver, spleen and kidneys in healthy mice (data not shown).

Macroscopically, multiple liver nodules were frequently observed in mice with liver tumour (4 out of 15; Table 1, Figure 2a). The number and size of the nodules varied. Microscopically, liver tumours showed various degrees of cellular atypia, from adenoma to HCC with occasional 'carcinoma in adenoma', suggesting ongoing progression. The expression of α-fetoprotein, a marker of human HCC, was detected in the tumours by immunohistochemical analyses (Figure 2b) and quantitative reverse transcription PCR (qRT-PCR) (Supplementary Figure 1). None of the tumours showed

Table 1 Frequencies of tumours observed in TNAP-AID and control mice

Genotype	*Mean age at killing (weeks)*	*HCC*	*Lymphoma*	*Lung cancer*	*Stomach cancer*
TNAP-AID (15)	88.5	26.7% (4)	40.0% (6)	6.7% (1)	6.7% (1)
AID-cTg (24)	89.9	0.0% (0)	29.2% (7)	0.0% (0)	0.0% (0)
TNAP-Cre (14)	88.4	0.0% (0)	0.0% (0)	0.0% (0)	0.0% (0)
WT (23)	89.1	0.0% (0)	17.4% (4)	0.0% (0)	0.0% (0)

Abbreviations: HCC, hepatocellular carcinoma; WT, wild type.
Frequencies were calculated from the numbers of mice with macroscopic tumours of the indicated organs at approximately 90 weeks of age. Numbers in parentheses are the number of individuals killed for tumour inspection (genotype column) and those with macroscopic tumours (right four columns).

nuclear localization of β-catenin protein (data not shown).

Sequences of some tumour suppressor genes and oncogenes in the tumours were determined. Significant numbers of mutations were observed in the *Trp53* gene encoding the p53 protein (Table 2). The non-transcribed region upstream of the promoter did not contain mutations, an observation that is consistent with the transcription dependence of mutagenesis by AID (Yoshikawa *et al.*, 2002). Majority of mutations were single-base substitutions with significant GC bias, another footprint of AID (Figure 3a) (Yoshikawa *et al.*, 2002). There was no significant correlation between the distribution of mutations and those of SHM hot spot motifs (RGYW/WRCY) and DNA secondary structures (Supplementary Figure 2). Interestingly, the mutation frequency was the highest in cancer tissues followed by non-cancerous TNAP-AID liver and lowest in normal liver of WT mice, which corresponds to the PCR error rate or the background rate in this assay. The increase in mutation frequency in HCC compared with non-cancerous liver was because of the increase in single-base insertion events mostly at the homonucleotide tracts, leading to frameshift mutations in the 5′-half of the coding region (Table 2 and Figure 3b). Most of TNAP-AID liver mutations occurred in the DNA-binding domain of p53, which is critical for its function (Table 3).

Although small volumes (approximately 50 mm^3) of normal and cancerous liver tissues were dissected for mutation analysis, the identified mutations were quite diverse, suggesting that the sampled tissue block contained multiple HCC nodules, each representing monoclonal expansion. Such heterogeneity was verified by two independent series of PCR, plasmid cloning and sequencing for the same sample: there were few overlaps of mutations. For example, 8 and 7 clones derived from HCC of mouse TA113 contained nonsynonymous point mutations out of sequenced 27 and 40 clones in the first and second experiment, respectively. The mutation patterns were completely different except C808G (R270G), which appeared thrice and once in the first and the second trial, respectively. Table 3 lists the combined results of the two experiments. The most frequent mutations were C790T(R264W) and C808G(R270G), the latter corresponding to one of the second most important mutational targets (R273) in human cancers (Figure 3b, top). Despite extensive sequencing, no mutations were found in *Myc*, *Pten* and *Cdkn2a* (p16 and $p19^{Arf}$) genes (Supplementary Figure 3). The *Trp53* mutation frequency in the thymus was significantly lower than in the liver of TNAP-AID mice, which is consistent with the lack of lethal T-cell lymphomagenesis (Table 2).

To determine why liver tumours developed, TNAP expression in various organs was examined by qRT-PCR in E14.5 embryos and 53- to 74-week-old adult mice of strain C57BL/6. TNAP was ubiquitously expressed at a relatively high level in the liver and intestine of the embryos and in the liver and testis of the adults (Figure 4a). In agreement with this wide distribution of TNAP expression, GFP expression in TNAP-AID mice was absent in most organs in adults (Figure 4c). The substantial levels of AID expression were confirmed by qRT-PCR (Figure 4b) and western blotting (Figure 4d) in various organs of the adult TNAP-AID mice but not of AID cTg mice. The presence of AID protein and loss of GFP were detected in the non-cancerous liver sections of TNAP-AID mice (Figure 5). Taken together, these findings suggest that constitutive AID expression in hepatic lineage, including fetal and adult liver, contributes to the high incidence of liver tumours.

As reported for AID transgenic mice with the ubiquitous promoter, lymphomas were observed in TNAP-AID mice (Table 1). Although the frequency of lymphomas in the TNAP-AID group was higher than those in the other groups, the differences between TNAP-AID and AID cTg mice ($P=0.508$) and those between TNAP-AID and WT mice ($P=0.150$) were not statistically significant. The survival curve analysis (Figure 1c) suggested that there was no significant difference between the TNAP-AID and TNAP-Cre groups ($P=0.515$), indicating that the lymphomas in TNAP-AID mice were less aggressive than those in the transgenic mice with ubiquitous AID expression. Histologically, the lymphomas in TNAP-AID mice exhibited nodular appearance, which was different from that of the diffusely infiltrating lymphoma that develops in the ubiquitous promoter-driven AID transgenic mice (data not shown). This difference suggests that different mechanisms underlie tumorigenesis of lymphoid cells between these mice. We confirmed that GFP expression and Cre-mediated excision of GFP occurred efficiently in CD3-positive T cells of AID cTg and TNAP-AID mice, respectively (Supplementary Figure 4). This suggests that AID is expressed in T cells of TNAP-AID mice.

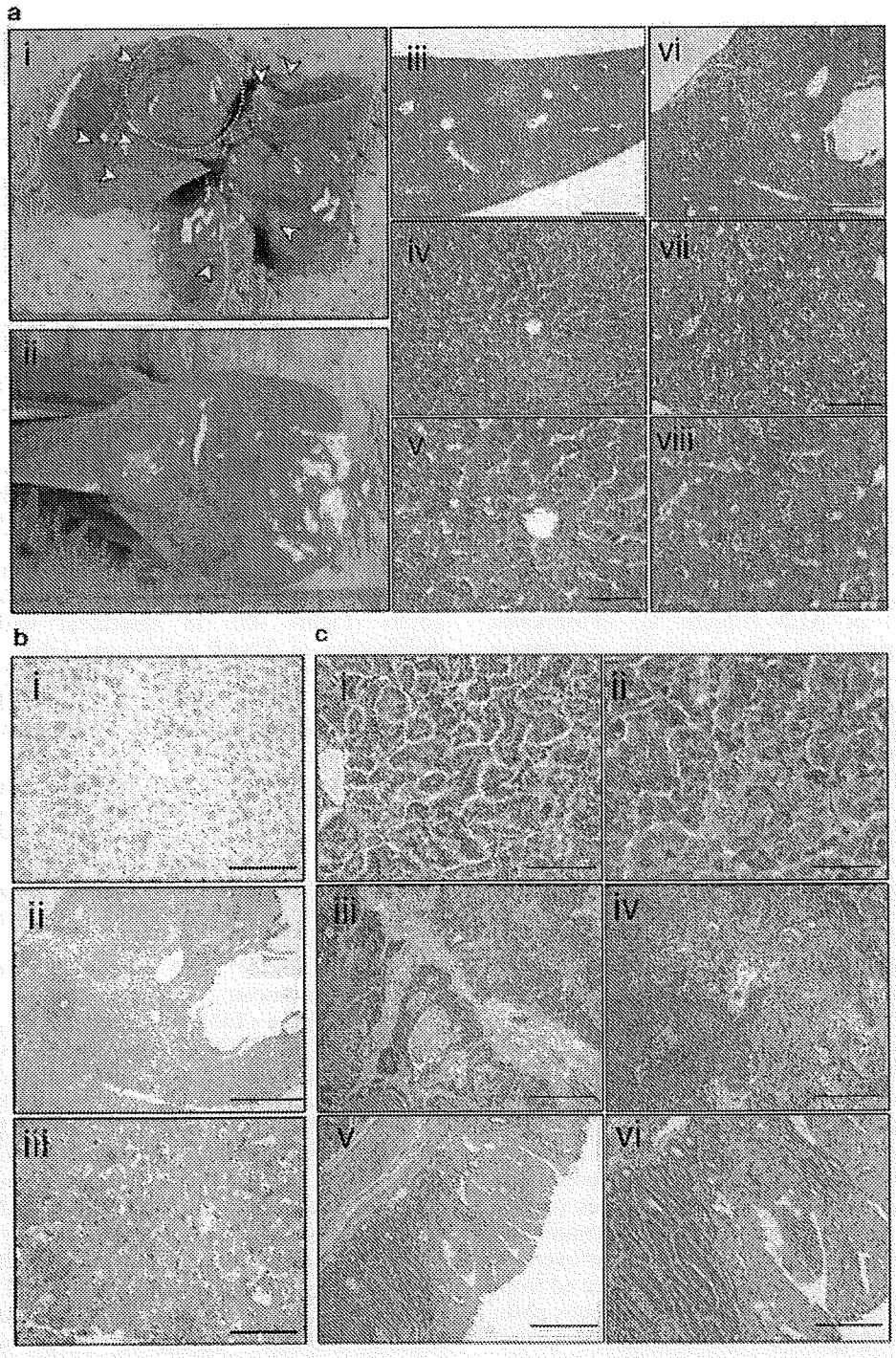

Figure 2 Tumours developed in TNAP-AID mice. (**a**) Macroscopic (i and ii) and microscopic (haematoxylin and eosin (HE) stain) images of HCC (i, ii, vi, vii and viii) that developed in a TNAP-AID mouse and non-cancerous liver of the same animal (iii, iv and v). In panel ai, arrowheads indicate liver tumour nodules. The largest nodule is encircled with a dotted line, and its cut surface is shown in panel aii). Scale bars are 1 mm (iii and iv), 500 μm (iv and vii) and 200 μm (v and viii). (**b**) Immunohistochemistry for α-fetoprotein of the normal liver (i) and HCC (ii and iii), which are serial sections of images shown in panel aiv, avi and aviii, respectively. Scale bars are 500 μm (i and iii) and 1 mm (ii). (**c**) Microscopic images (HE stain) of cancer of the lung (i and ii) and the stomach (iii and iv, squamous cell carcinoma; v and vi, adenocarcinoma). Scale bars are 200 μm (i, iv and vi), 100 μm (ii) and 500 μm (iii and v).

Table 2 *Trp53* gene mutation profiles in liver and HCC of TNAP-AID mice

Target	*Genotype*	*WT*	*TNAP-AID*	*HCC*	*Gastric cancer*	*Thymus*
	Tissue	*Normal liver*	*Non-cancerous liver*			
Transcribed region	Mutated/total clones	4/48	11/49	33/112	7/34	0/21
	Mutated (pm:ins:del)/total bases	4 (2:1:1)/52 487	12 (10:2:0)/55 321	42 (27:13:2)/127 674	9 (5:3:1)/38 789	0/24 446
	Mutation frequency $\times 10^4$	0.76	2.17	3.29	2.32	0.00
Non-transcribed region	Mutated/total clones	0/16	0/15	0/16		
	Mutated (pm:ins:del)/total bases	0/13 828	0/12 613	0/13 947		
	Mutation frequency $\times 10^4$	0.00	0.00	0.00		

Abbreviations: HCC, hepatocellular carcinoma; WT, wild type.
Mutation frequency of the transcribed and non-transcribed regions of the *Trp53* gene of the normal liver from two WT mice (87- and 89-week-old) and non-cancerous liver, HCC and thymic tissues from three TNAP-AID mice (92- to 94-week-old). Mutated base numbers are shown with numbers of point mutations (pm), insertions (ins) and deletions (del) in parentheses.

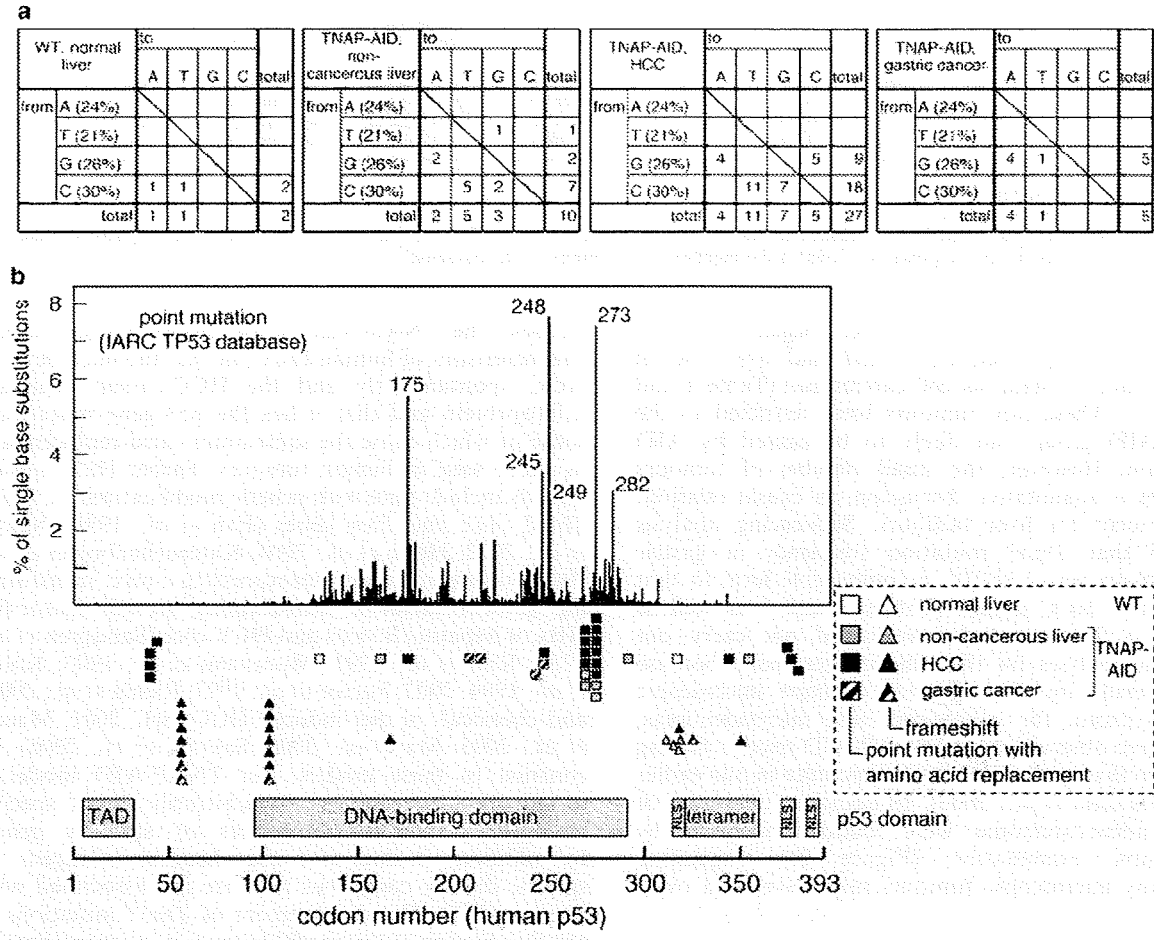

Figure 3 *Trp53* gene mutation profiles in liver and HCC of TNAP-AID mice. (a) Base substitution patterns seen in liver of WT mice (left), non-cancerous liver of TNAP-AID mice (centre) and HCC of TNAP-AID mice (right) extracted from the same data sets as those used for the mutation frequency analysis in Table 2. Percentages in parentheses are compositions of the indicated bases in the sequenced region. (b) Top: Distribution of *TP53* somatic mutations in human cancer, reproduced from the IARC TP53 Database (version R12), November 2007 (http://www-p53.iarc.fr/) (Petitjean *et al.*, 2007). Middle: Distribution of mouse *Trp53* mutations found in WT and TNAP-AID mouse liver. Codon positions are converted into human equivalents. Squares and triangles indicate point mutations with amino acid replacements and frameshifts, respectively. Open, grey, filled and hatched symbols indicate normal liver of WT mice, non-cancerous liver, HCC and gastric cancer of TNAP-AID mice, respectively. Bottom: p53 domain structure with transactivation (TAD), DNA-binding and tetramerization domains and nuclear localization signal (NLS).

Table 3 Predicted amino acid replacements observed in three TNAP-AID mice (TA113, TA114 and TA128), corresponding human mutations and affected domains of p53

Tissue	*Mutation*		*Mouse ID*	*Mutated/total clone*	*Human-equivalent codon*	*Domain*	*Functional assays*[a]		*Count*[a]
	Nucleotide	*Codon*					*Transactivation class*	*Structure-based prediction*	
TNAP-AID, non-cancerous liver	G472A	A158T	TA113	1/26	A161T	DNA binding	Partially functional	Non-functional	73
	C790T	R264W	TA128	2/23	R267W	DNA binding	Non-functional	Non-functional	25
	C808G	R270G	TA128	2/23	R273G	DNA binding	Non-functional	Non-functional	14
	G860A	R287H	TA113	1/26	R290H	DNA binding	Supertrans	NA	29
	C1049T	A350V	TA113	1/26	A353V	Tetramerization	Supertrans	NA	0
TNAP-AID, HCC	G119C	C40S	TA113	2/67	None	Transactivation	NA	NA	NA
			TA114	1/33					
	G127A	D43N	TA113	1/67	D42N	Transactivation	Functional	NA	0
	C532T	R178C	TA114	1/33	R175C	DNA binding	Partially functional	Non-functional	24
	G729A	M243I	TA113	1/67	M246I	DNA binding	Non-functional	Functional	32
	C790T	R264W	TA113	3/67	R267W	DNA binding	Non-functional	Non-functional	25
			TA114	1/33					
	C808G	R270G	TA113	4/67	R273G	DNA binding	Non-functional	Non-functional	14
			TA114	2/33					
	G1020C	E340D	TA113	1/67	E343D	Tetramerization	Functional	NA	0
	G1112A	G371D	TA113	1/67	G374D	Regulation/NLS	Functional	NA	0
	C1118G	S373C	TA113	1/67	S376C	Regulation/NLS	Functional	NA	0
	G1127C	R376P	TA113	1/67	R379P	Regulation	Partially functional	NA	0
TNAP-AID, gastric cancer	G613T	D205Y	TA114	1/34	D208Y	DNA binding	Non-functional	Functional	1
	G629A	R210H	TA114	1/34	R213Q	DNA binding	Non-functional	Non-functional	34
	G716A	C239Y	TA114	1/34	C242Y	DNA binding	Non-functional	Non-functional	51
	G729A	M243I	TA114	1/34	M246I	DNA binding	Non-functional	Functional	32

Abbreviation: NA, data not available.
For details, visit the IARC website.
[a]Based on the data presented in the IARC website and described in the legend of Figure 3. Functional assays are predicted as impacts of mutations in yeast assays and structural computation. Count is the number of the entries in the database.

Macroscopic tumours of other organs included one case of lung adenocarcinoma and one case of gastric cancer (squamous cell carcinoma) (Table 1 and Figure 2c). These rare tumours were restricted to the TNAP-AID group and likely to be caused by AID expression. However, the small number of tumours precludes a quantitative discussion on causal relationships, except for liver tumours. Sequencing analysis revealed that *Trp53* mutation frequency in gastric cancer tissue was $2.32/10^4$, a comparable level to that observed in HCC tissues (Tables 2 and 3 as well as Figure 3). Unfortunately, we could not carry out mutation analyses on the lung cancer tissue because of its small size. We did not examine microscopic tumours except for subpleural lung microadenomas, which were observed in the TNAP-AID mice, a finding similar to that in the AID transgenic mice in our earlier study (Okazaki *et al.*, 2003). In addition, two cases of gastric adenocarcinoma were found incidentally by microscopic examination (Figure 2c), suggesting that many microscopic tumours may have been overlooked.

Discussion

Here we describe TNAP-AID mice as a novel model of hepatocarcinogenesis, which occurs as a result of the accumulation of mutations in chronically inflamed liver in humans, often caused by infection with hepatitis viruses. The TNAP-AID mouse model exhibits several characteristics of human HCC, in that the mice develop HCC spontaneously and the HCC tissue expresses α-fetoprotein and that it has the p53 gene mutations, some of which cause the same amino acid replacements as those seen in human tumours. Earlier HCC mouse models include mice with genetic modifications of *Lkb1*, *Mdr2*, *Aox* and *Pten* genes (Fan *et al.*, 1998; Nakau *et al.*, 2002; Horie *et al.*, 2004; Katzenellenbogen *et al.*, 2006), transgenic mice overexpressing c-myc, transforming growth factor-α, transforming growth factor-β1, HBx of hepatitis B virus and HCV core (Sandgren *et al.*, 1989; Kim *et al.*, 1991; Murakami *et al.*, 1993; Koike *et al.*, 1994, 2002; Factor *et al.*, 1997; Riehle *et al.*, 2008) and chemical- or diet-induced HCC (Sell, 2001; Maeda *et al.*, 2005; Ma *et al.*, 2006; Sakurai *et al.*, 2006). In contrast to these models, our TNAP-AID model is unique because it does not arbitrarily target specific oncogenes, tumour suppressors or stability genes. In addition, it does not use chemical mutagens or specific dietary conditions that are not associated with human HCC. The development of *Trp53* mutations is another feature of this model because it is unprecedented in any earlier mouse HCC models as mentioned above.

Liver tumours were occasionally observed in our earlier AID transgenic mice (Endo *et al.*, 2007). However, it was difficult to use these mice as a liver tumour model because of early death from lethal lymphomas. Trials to detect *Trp53* mutations in the liver tumour failed (data not shown). Even the T-cell

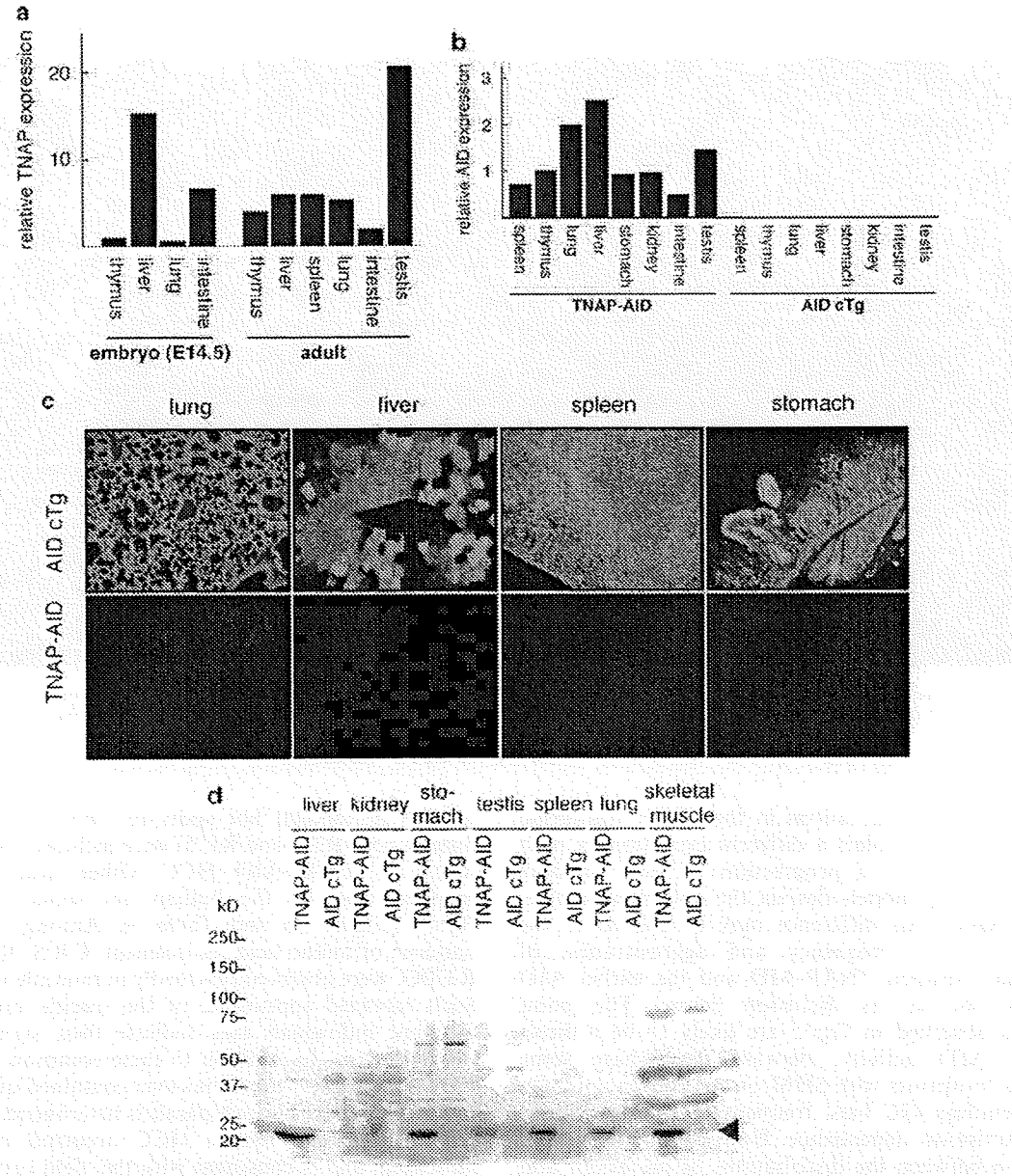

Figure 4 Expression analysis of TNAP-AID mice. (**a**) Results of qRT-PCR for TNAP gene (*Akp2*) calibrated by the amount of ribosomal 18S RNA for indicated organs of adult mice (53- and 74-week-old) and four E14.5 embryos. The graph shows average results for the indicated groups. (**b**) Results of qRT-PCR for transgene-derived AID expression. (**c**) GFP fluorescence in frozen sections of GFP from the indicated organs and animals. A mosaic pattern of GFP expression in the liver of AID cTg mice was always observed, which may be attributed to the integration site of the transgene. (**d**) Western blot analysis using anti-AID monoclonal antibody MAID-1 for the lysates of indicated organs of 42-week-old TNAP-AID and AID cTg mice. Arrowhead indicates the position of the AID band. Comparable intensities of nonspecific bands indicate equal loading of extracts between TNAP-AID and AID cTg lanes.

lymphomas that developed in the earlier AID transgenic mice did not harbour *Trp53* mutations (Kotani *et al.*, 2005). Therefore, the TNAP-AID mouse model is the first model in which *Trp53* mutations can be detected unequivocally in non-cancerous tissues as well as in cancerous tissues that express AID. In spite of these differences, the two independent AID transgenic mice lines commonly developed liver tumours, making it unlikely that liver tumours in TNAP-AID mice are ascribed to unexpected variables such as the transgene integration sites and the segregation of relevant loci upon crossing of mice with different genetic backgrounds. However, the possibility that these variables somewhat modified the tumour frequency cannot be excluded.

The overlap of mutational hot spots between TNAP-AID and human HCC (Table 3 and Figure 3b) suggests that these mutations induced by AID have critical roles.

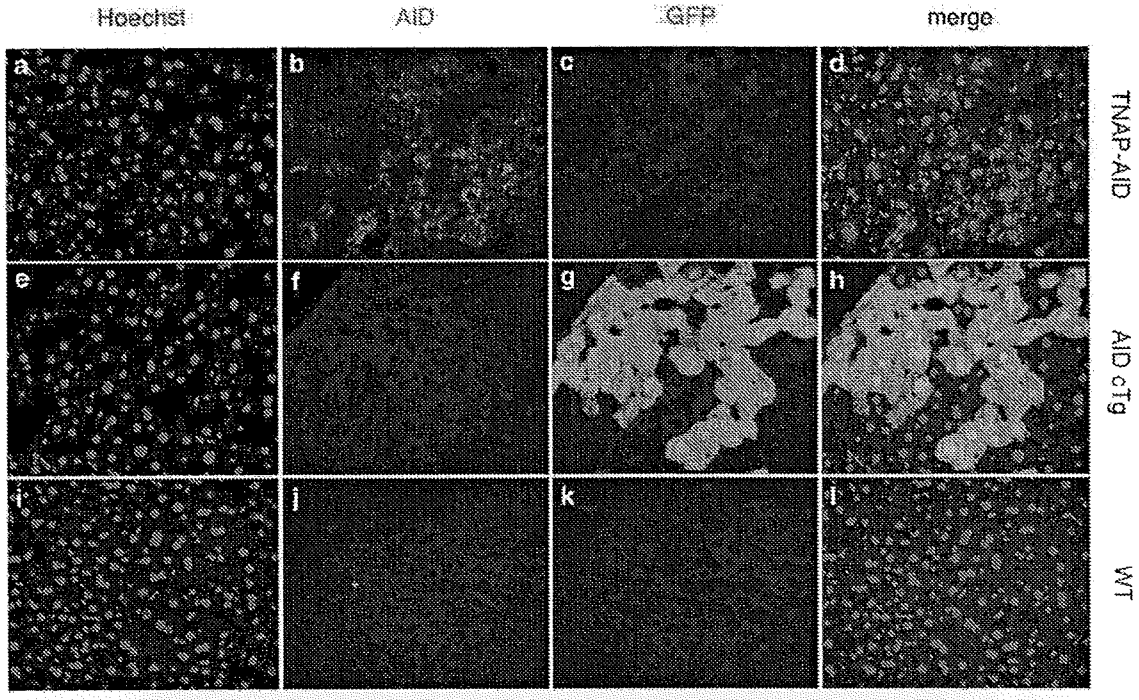

Figure 5 Immunohistochemical analysis of frozen liver sections from TNAP-AID (**a–d**), AID cTg (**e–h**) and WT (**i–l**) mice. (**a**, **e** and **i**) Hoechst 33342 staining; (**b**, **f** and **j**) AID immunostaining; (**c**, **g** and **k**) GFP fluorescence; (**d**, **h** and **l**) merge of the three colours.

The lack of *Trp53* mutations in the earlier transgenic mouse model may reflect a different evolutionary path from the initiation to progression of liver tumours between the two models despite the common involvement of AID. This difference may be related to the difference in the frequency and aggressiveness of lymphomas between TNAP-AID and the earlier AID transgenic mouse, as discussed below. The point mutations observed in *Trp53* are likely to be a direct effect of AID activity, because they share some molecular footprints with SHM of the immunoglobulin genes, including GC bias, frequent C-to-T transitions and transcription dependence. However, there was no correlation between the distributions of mutations and SHM hot spot motifs or DNA secondary structures in the *Trp53* sequence. As these parameters show only weak association even for SHM, the small numbers of point mutations observed in this study may not be sufficient to achieve statistical significance. On the other hand, single-base insertions causing frameshifts in *Trp53* were frequently observed in HCC but not in the non-cancerous liver of TNAP-AID mice. As single-base insertions are relatively rare in SHM induced by AID, these might be caused by genetic instability (for example, impaired mismatch repair) acquired during the progression of the tumours.

The presence of mutations in non-cancerous tissue expressing AID is reminiscent of a study on human patients with chronic hepatitis (Kou *et al.*, 2006), together suggesting a causal role of AID in tumorigenesis. It is noteworthy that the mutations corresponding to two mutational hot spots in *TP53* gene encoding human p53 (R273 and R175) were included in mutations found in TNAP-AID HCC. Other mutations were mapped close to the human hot spots (M246 and R267) (Figure 3b and Table 3). Among them three patterns of amino acid replacement, C40S, R264W and R270G, were observed repeatedly in multiple individuals. Such repeated appearance of the specific mutations in different individuals may indicate their significance in tumorigenesis. In addition to these common mutations, HCC and the non-cancerous liver contained quite diverse mutation patterns, which parallels heterogeneity of *TP53* mutations within human HCC occurred in a single individual and is consistent with the 'field cancerization' model (Thorgeirsson and Grisham, 2002).

The utility of the TNAP-AID mouse as a human HCC model depends partly on the lack of lethal lymphomas that were observed in almost all AID transgenic mice in our earlier study. To examine the reason why lymphomas were infrequent and less aggressive in the TNAP-AID model, mutations caused by AID and its expression in T lymphocytes of TNAP-AID mice were analysed by sequencing the *Trp53* coding sequence (Table 2) and flow cytometry (Supplementary Figure 4). From these analyses, it was found that *Trp53* was not mutated, but AID was expressed in the thymocytes of the TNAP-AID mice. The level of AID expression in the thymus of TNAP-AID mice was half than that seen in the earlier AID transgenic line in a qRT-PCR analysis (data not shown). We speculate that the difference in the levels of AID expression in T cells

may be one of the reasons for this, although the difference in the genetic background (C57BL/6:129/Sv hybrid versus pure C57BL/6) cannot be excluded.

The TNAP-AID mice did not develop germ cell tumours despite the expression of AID in the testes (Figure 4d) and the absence of GFP in the seminiferous tubules and oocytes of the ovaries (data not shown). We reported earlier the lack of lymphomagenesis in B-cell-specific AID transgenic mice obtained by crossing the same AID cTg line with CD19-Cre mice (Muto *et al.*, 2006), suggesting that some protective mechanism might exist in B cells, which have physiological expression of AID. A similar reason might apply to germ cells because AID has been reported to be expressed physiologically in the human testis (Schreck *et al.*, 2006) and mouse ovary (Morgan *et al.*, 2004).

To conclude, we generated a new line of AID transgenic mice that develop HCC but not lethal T-cell lymphoma. We consider that the TNAP-AID mouse model is useful for human HCC studies because it has been shown that AID is induced in the human pre-cancerous conditions of chronic hepatitis and cirrhosis (Kou *et al.*, 2006). The relatively long latency before HCC development in this model is reasonable, considering that it is a physiological recapitulation of a human tumour phenotype that takes decades to develop.

Materials and methods

Mice

The AID cTg mice (line 20) on a C57BL/6 background (Muto *et al.*, 2006) were self-crossed to obtain homozygous transgenic mice, which were maintained in a specific pathogen-free facility at the Kyoto University Faculty of Medicine and Shiga Medical Center. This mouse line has been deposited at the Riken Bioresource Center (Tsukuba, Japan; No. RBRC00892). The TNAP-Cre mice (Lomeli *et al.*, 2000) were gifted by Dr Andras Nagy (Mount Sinai Hospital, Toronto, Canada) and maintained by self-crossing between the heterozygous mice. C57BL/6 mice were purchased from Shimizu Laboratory Supplies Co., Ltd (Kyoto, Japan). All mice were fed *ad libitum* and were killed by cervical dislocation for censoring, or observed until spontaneous death. Upon censoring and spontaneous death, the numbers of macroscopic tumours were counted after laparotomy and thoracotomy. Kaplan–Meier survival curves were analysed using Prism 4.0 software (Graphpad, San Diego, CA, USA). All animal experiments were approved by the Ethical Committee for Animal Experiments and performed under the Guidelines for Animal Experiments of Kyoto University and Shiga Medical Center.

Histology and immunohistochemistry

Paraffin-embedded mouse organs were sectioned and stained with haematoxylin and eosin. α-Fetoprotein was detected using anti-α-fetoprotein antibody (Dako, Glostrup, Denmark) and an ABC kit (Vector, Burlingame, CA, USA) for paraffin-embedded sections of formalin-fixed liver. For AID immunostaining, freshly isolated liver was fixed in 4% paraformaldehyde in phosphate-buffered saline on ice for 2 h and immersed in 30% sucrose for 18 h. After embedding in OCT compound (Sakura Fineteck Japan, Tokyo, Japan) in liquid nitrogen, 8-μm sections were sliced and mounted on glass slides. Hoechst 33342 dye was used to visualize nuclei. AID protein was detected using the monoclonal anti-AID antibody, MAID-2 (Tsuji *et al.*, 2008), with peroxidase-labelled donkey F(ab')2 anti-rat IgG (Jackson ImmunoResearch, West Grove, PA, USA) and signal amplification using TSA Plus DNP and TSA Plus TMR kits (Perkin Elmer, Waltham, MA, USA). Images taken with a fluorescence microscope (DM5000B; Leica, Wetzlar, Germany) were merged using Photoshop (Adobe, San Jose, CA, USA).

Mutation analysis

Cancerous and non-cancerous liver tissues of approximate volume of 50 mm^3 were macroscopically dissected, frozen in liquid nitrogen and powdered with a frozen-cell crusher (Cryo-press; Microtec, Funabashi, Japan). Genomic DNA and total RNA were extracted using the QIAamp DNA Mini kit (Qiagen, Duesseldorf, Germany) and the QuickGene kit (Fuji, Tokyo, Japan) from liquid nitrogen-frozen tissues that had been dissected macroscopically from non-cancerous livers and cancerous nodules. Sequencing of *Trp53* was performed as described earlier (Matsumoto *et al.*, 2007) except for primers for the non-transcribed regions, sequences of which are shown in Supplementary Figure 5. Mutations of the *Myc*, *Pten* and *Cdkn2a* genes were analysed as described (Matsumoto *et al.*, 2007) except for primers, sequences of which are shown in Supplementary Figure 5. Statistical significance was assessed by Fisher's exact test using Stata 8.2 software (Stata Corp, College Station, TX, USA). Searching for SHM hot spot motifs and DNA secondary structure analyses were performed using GENETYX-MAC 14 (Genetyx Corp., Tokyo, Japan) and mfold software (Zuker, 2003), respectively.

qRT-PCR

cDNA was synthesized using the iScript kit (Bio-Rad, Hercules, CA, USA). Quantitative PCR (qPCR) was performed using QuantiTect reagent (Qiagen) and a real-time thermal cycler (Mx3000P; Stratagene, La Jolla, CA, USA). Oligonucleotide sequences are shown in Supplementary Figure 5.

Western blotting

Mouse organs were dissected, frozen in liquid nitrogen and powdered with a frozen-cell crusher (Cryo-press). Proteins were extracted from the tissue powder using 10 mM sodium phosphate (pH 6.8), 200 mM NaCl, 1.5 mM $MgCl_2$ and 0.2 mM EDTA with a protease inhibitor cocktail (Complete: Roche Diagnostics, Mannheim, Germany). Protein of 100 μg per lane was applied to a 5–20% polyacrylamide gel (Bio-Rad), electrophoresed and blotted on to Hybond P membrane (GE Healthcare, Buckinghamshire, UK). Signals were generated using peroxidase-labelled anti-rat IgG (Jackson ImmunoResearch) and the ECL Plus system (GE Healthcare) and detected with a LAS-3000 mini image analysis system (Fuji).

Acknowledgements

We thank Dr Andras Nagy for his generous gift of TNAP-Cre mice, Dr Takashi Shinohara for suggesting the choice of the Cre mouse strain, Dr Yoshinobu Toda for the preparation of tissue sections and Dr Masayuki Tsuji for technical help with the immunohistochemical analyses. We also thank Dr Sidonia Fagarasan for critical reading of the manuscript and discussions. This study was supported by Grant-in-Aid for Scientific Research (17013042 and 18390122) and the Takeda Science Foundation.

References

Endo Y, Marusawa H, Kinoshita K, Morisawa T, Sakurai T, Okazaki IM *et al.* (2007). Expression of activation-induced cytidine deaminase in human hepatocytes via NF-kappaB signaling. *Oncogene* **26**: 5587–5595.

Factor VM, Kao CY, Santoni-Rugiu E, Woitach JT, Jensen MR, Thorgeirsson SS. (1997). Constitutive expression of mature transforming growth factor beta1 in the liver accelerates hepatocarcinogenesis in transgenic mice. *Cancer Res* **57**: 2089–2095.

Fan CY, Pan J, Usuda N, Yeldandi AV, Rao MS, Reddy JK. (1998). Steatohepatitis, spontaneous peroxisome proliferation and liver tumors in mice lacking peroxisomal fatty acyl-CoA oxidase. Implications for peroxisome proliferator-activated receptor alpha natural ligand metabolism. *J Biol Chem* **273**: 15639–15645.

Honjo T, Kinoshita K, Muramatsu M. (2002). Molecular mechanism of class switch recombination: linkage with somatic hypermutation. *Annu Rev Immunol* **20**: 165–196.

Horie Y, Suzuki A, Kataoka E, Sasaki T, Hamada K, Sasaki J *et al.* (2004). Hepatocyte-specific Pten deficiency results in steatohepatitis and hepatocellular carcinomas. *J Clin Invest* **113**: 1774–1783.

Katzenellenbogen M, Pappo O, Barash H, Klopstock N, Mizrahi L, Olam D *et al.* (2006). Multiple adaptive mechanisms to chronic liver disease revealed at early stages of liver carcinogenesis in the Mdr2-knockout mice. *Cancer Res* **66**: 4001–4010.

Kim CM, Koike K, Saito I, Miyamura T, Jay G. (1991). HBx gene of hepatitis B virus induces liver cancer in transgenic mice. *Nature* **351**: 317–320.

Kinoshita K, Nonaka T. (2006). The dark side of activation-induced cytidine deaminase: relationship with leukemia and beyond. *Int J Hematol* **83**: 201–207.

Koike K, Moriya K, Iino S, Yotsuyanagi H, Endo Y, Miyamura T *et al.* (1994). High-level expression of hepatitis B virus HBx gene and hepatocarcinogenesis in transgenic mice. *Hepatology* **19**: 810–819.

Koike K, Moriya K, Kimura S. (2002). Role of hepatitis C virus in the development of hepatocellular carcinoma: transgenic approach to viral hepatocarcinogenesis. *J Gastroenterol Hepatol* **17**: 394–400.

Komori J, Marusawa H, Machimoto T, Endo Y, Kinoshita K, Kou T *et al.* (2008). Activation-induced cytidine deaminase links bile duct inflammation to human cholangiocarcinoma. *Hepatology* **47**: 888–896.

Kotani A, Okazaki IM, Muramatsu M, Kinoshita K, Begum NA, Nakajima T *et al.* (2005). A target selection of somatic hypermutations is regulated similarly between T and B cells upon activation-induced cytidine deaminase expression. *Proc Natl Acad Sci USA* **102**: 4506–4511.

Kou T, Marusawa H, Kinoshita K, Endo Y, Okazaki IM, Ueda Y *et al.* (2006). Expression of activation-induced cytidine deaminase in human hepatocytes during hepatocarcinogenesis. *Int J Cancer* **120**: 469–476.

Kues WA, Petersen B, Mysegades W, Carnwath JW, Niemann H. (2005). Isolation of murine and porcine fetal stem cells from somatic tissue. *Biol Reprod* **72**: 1020–1028.

Lomeli H, Ramos-Mejia V, Gertsenstein M, Lobe CG, Nagy A. (2000). Targeted insertion of Cre recombinase into the TNAP gene: excision in primordial germ cells. *Genesis* **26**: 116–117.

Ma W, Xia X, Stafford LJ, Yu C, Wang F, LeSage G *et al.* (2006). Expression of GCIP in transgenic mice decreases susceptibility to chemical hepatocarcinogenesis. *Oncogene* **25**: 4207–4216.

Maeda S, Kamata H, Luo JL, Leffert H, Karin M. (2005). IKKbeta couples hepatocyte death to cytokine-driven compensatory proliferation that promotes chemical hepatocarcinogenesis. *Cell* **121**: 977–990.

Marusawa H. (2008). Aberrant AID expression and human cancer development. *Int J Biochem Cell Biol* **40**: 1399–1402.

Matsumoto Y, Marusawa H, Kinoshita K, Endo Y, Kou T, Morisawa T *et al.* (2007). Helicobacter pylori infection triggers aberrant expression of activation-induced cytidine deaminase in gastric epithelium. *Nat Med* **13**: 470–476.

Morgan HD, Dean W, Coker HA, Reik W, Petersen-Mahrt SK. (2004). Activation-induced cytidine deaminase deaminates 5-methylcytosine in DNA and is expressed in pluripotent tissues: implications for epigenetic reprogramming. *J Biol Chem* **279**: 52353–52360.

Murakami H, Sanderson ND, Nagy P, Marino PA, Merlino G, Thorgeirsson SS. (1993). Transgenic mouse model for synergistic effects of nuclear oncogenes and growth factors in tumorigenesis: interaction of c-myc and transforming growth factor alpha in hepatic oncogenesis. *Cancer Res* **53**: 1719–1723.

Muto T, Okazaki IM, Yamada S, Tanaka Y, Kinoshita K, Muramatsu M *et al.* (2006). Negative regulation of activation-induced cytidine deaminase in B cells. *Proc Natl Acad Sci USA* **103**: 2752–2757.

Nakau M, Miyoshi H, Seldin MF, Imamura M, Oshima M, Taketo MM. (2002). Hepatocellular carcinoma caused by loss of heterozygosity in Lkb1 gene knockout mice. *Cancer Res* **62**: 4549–4553.

Okazaki IM, Hiai H, Kakazu N, Yamada S, Muramatsu M, Kinoshita K *et al.* (2003). Constitutive expression of AID leads to tumorigenesis. *J Exp Med* **197**: 1173–1181.

Petitjean A, Mathe E, Kato S, Ishioka C, Tavtigian SV, Hainaut P *et al.* (2007). Impact of mutant p53 functional properties on TP53 mutation patterns and tumor phenotype: lessons from recent developments in the IARC TP53 database. *Hum Mutat* **28**: 622–629.

Riehle KJ, Campbell JS, McMahan RS, Johnson MM, Beyer RP, Bammler TK *et al.* (2008). Regulation of liver regeneration and hepatocarcinogenesis by suppressor of cytokine signaling 3. *J Exp Med* **205**: 91–103.

Sakurai T, Maeda S, Chang L, Karin M. (2006). Loss of hepatic NF-kappa B activity enhances chemical hepatocarcinogenesis through sustained c-Jun N-terminal kinase 1 activation. *Proc Natl Acad Sci USA* **103**: 10544–10551.

Sandgren EP, Quaife CJ, Pinkert CA, Palmiter RD, Brinster RL. (1989). Oncogene-induced liver neoplasia in transgenic mice. *Oncogene* **4**: 715–724.

Schreck S, Buettner M, Kremmer E, Bogdan M, Herbst H, Niedobitek G. (2006). Activation-induced cytidine deaminase (AID) is expressed in normal spermatogenesis but only infrequently in testicular germ cell tumours. *J Pathol* **210**: 26–31.

Sell S. (2001). Heterogeneity and plasticity of hepatocyte lineage cells. *Hepatology* **33**: 738–750.

Thorgeirsson SS, Grisham JW. (2002). Molecular pathogenesis of human hepatocellular carcinoma. *Nat Genet* **31**: 339–346.

Tsuji M, Suzuki K, Kitamura H, Maruya M, Kinoshita K, Ivanov II *et al.* (2008). Requirement for lymphoid tissue-inducer cells in isolated follicle formation and T cell-independent immunoglobulin a generation in the gut. *Immunity* **29**: 261–271.

Urven LE, Weng DE, Schumaker AL, Gearhart JD, McCarrey JR. (1993). Differential gene expression in fetal mouse germ cells. *Biol Reprod* **48**: 564–574.

Vogelstein B, Kinzler KW. (2004). Cancer genes and the pathways they control. *Nat Med* **10**: 789–799.

Wang L, Duan E, Sung LY, Jeong BS, Yang X, Tian XC. (2005). Generation and characterization of pluripotent stem cells from cloned bovine embryos. *Biol Reprod* **73**: 149–155.

Yoshikawa K, Okazaki IM, Eto T, Kinoshita K, Muramatsu M, Nagaoka H *et al.* (2002). AID enzyme-induced hypermutation in an actively transcribed gene in fibroblasts. *Science* **296**: 2033–2036.

Zuker M. (2003). Mfold web server for nucleic acid folding and hybridization prediction. *Nucleic Acids Res* **31**: 3406–3415.

Supplementary Information accompanies the paper on the Oncogene website (http://www.nature.com/onc)

Journal of Viral Hepatitis, 2009, **16**, 388–396 doi:10.1111/j.1365-2893.2009.01095.x

Association of genetic polymorphisms with interferon-induced haematologic adverse effects in chronic hepatitis C patients

M. Wada,[1] H. Marusawa,[1] R. Yamada,[2] A. Nasu,[1] Y. Osaki,[3] M. Kudo,[4] M. Nabeshima,[5] Y. Fukuda,[6] T. Chiba[1] and F. Matsuda[2] [1]*Department of Gastroenterology and Hepatology,* [2]*Center of Genomic Medicine, Graduate School of Medicine, Kyoto University, Kyoto, Japan;* [3]*Department of Gastroenterology and Hepatology, Osaka Red Cross Hospital, Osaka, Japan;* [4]*Department of Gastroenterology and Hepatology, Kinki University, Osaka, Japan;* [5]*Department of Gastroenterology, Nara Hospital, Kinki University, Nara, Japan; and* [6]*Department of Laboratory Science, School of Health Science, Faculty of Medicine, Kyoto University, Kyoto, Japan*

Received August 2008; accepted for publication November 2008

SUMMARY. Interferon (IFN)-based combination therapy with ribavirin has become the gold standard for the treatment of chronic hepatitis C virus infection. Haematologic toxicities, such as neutropenia, thrombocytopenia, and anaemia, however, frequently cause poor treatment tolerance, resulting in poor therapeutic efficacy. The aim of this study was to identify host genetic polymorphisms associated with the efficacy or haematologic toxicity of IFN-based combination therapy in chronic hepatitis C patients. We performed comprehensive single nucleotide polymorphism detection in all exonic regions of the 12 genes involved in the IFN signalling pathway in 32 healthy Japanese volunteers. Of 167 identified polymorphisms, 35 were genotyped and tested for an association with the efficacy or toxicity of IFN plus ribavirin therapy in 240 chronic hepatitis C patients. Multiple logistic regression analysis revealed that low viral load, viral genotypes 2 and 3, and a lower degree of liver fibrosis, but none of the genetic polymorphisms, were significantly associated with a sustained virologic response. In contrast to efficacy, multiple linear regression analyses demonstrated that two polymorphisms (*IFNAR1* 10848-A/G and *STAT2* 4757-G/T) were significantly associated with IFN-induced neutropenia ($P = 0.013$ and $P = 0.011$, respectively). Thrombocytopenia was associated with the *IRF7* 789-G/A ($P = 0.031$). In conclusion, genetic polymorphisms in IFN signalling pathway-related genes were associated with IFN-induced neutropenia and thrombocytopenia in chronic hepatitis C patients. In contrast to toxicity, the efficacy of IFN-based therapy was largely dependent on viral factors and degree of liver fibrosis.

Keywords: haematologic adverse effect, hepatitis C, interferon, single nucleotide polymorphism, sustained virologic response.

INTRODUCTION

Hepatitis C virus (HCV) infects an estimated 170 million people worldwide [1] and is a leading cause of chronic hepatitis, liver cirrhosis, and primary hepatocellular carcinoma [2]. Currently, combination therapy with ribavirin (RBV) and either conventional interferon (IFN)-α or pegylated-IFN-α (peg-IFN-α) is the gold standard of treatment for chronic HCV infection [3,4], but the overall rate of a sustained virologic response (SVR) with these therapies ranges from only 54% to 63% [5–7]. The limited therapeutic efficacy might be due to the poor virologic response in some patients or to adverse effects of the IFN-based therapy, leading to low treatment tolerance [5,6].

Predictive factors associated with a virologic response to IFN-based therapy include viral and host factors. Several studies have recently reported a possible association between the efficacy of IFN-based therapy and polymorphisms in genes encoding cytokines, chemokines, or their receptors [8–14]. The reported single nucleotide polymorphisms (SNPs) associated with a virologic response to IFN-based therapy include the *IFNAR1* [8], *IL-10* [9,10], *TNF-α* [11], *IFN-γ* [12], *CCR5* [13], *osteopontin* [14] and *TLR7* [15] genes. These data, however, are controversial and inconclusive, because most of the previous studies analysed a selected single target gene. Indeed, such limited evaluation of only one or two SNPs might not be sufficient in determining association of genetic polymorphisms with a virologic response to IFN-based therapy. Moreover, few studies have involved patients treated with combination therapy using peg-IFN-α and RBV [16,17].

Abbreviations: ALT, alanine aminotransferase; CI, confidence interval; HCV, hepatitis C virus; IFN, interferon; OR, odds ratio; PCR, polymerase chain reaction; RBV, ribavirin; SNP, single nucleotide polymorphism; SVR, sustained virologic response.

Correspondence: Hiroyuki Marusawa, MD, PhD, Department of Gastroenterology and Hepatology, Graduate School of Medicine, Kyoto University, 54 Kawahara-cho, Shogoin, Sakyo-ku, Kyoto 606-8507, Japan. E-mail: maru@kuhp.kyoto-u.ac.jp

Among the side effects of IFN plus RBV combination therapy, haematologic toxicities are frequently observed and sometimes treatment must be discontinued or the drug dose reduced, resulting in reduced efficacy of the combination therapy [5,6,18]. However, the mechanisms and predictive factors in the occurrence of these adverse effects, especially the critical decrease in blood cell count, are not clear at present.

Many studies have clarified the molecular pathway of action of IFN in detail [4,19,20]. Binding of IFN-α to its receptor induces IFNAR1 and IFNAR2 dimerization, followed by the activation of IFNAR-associated tyrosine kinases (JAK1 and TYK2). These tyrosine kinases phosphorylate STAT1 and STAT2 monomers, leading to the induction of multiple IFN-stimulated genes. Moreover, type I IFNs induce IRF7 and IRF3, which are responsible for type 1 IFN induction mediated by the virus or Toll like receptors [21]. On the other hand, the mechanisms of IFN induction in response to viral infection were recently determined [22,23]. In HCV-infected cells, the cytoplasmic RNA helicase, RIG-I, recognizes the viral dsRNA and interacts with IPS-1, leading to activation of the transcription factors, IRF3 and NF-kB, which in turn transcribe type I IFN genes. In contrast, IRF2 negatively regulates the IFN signalling pathway and recent studies suggest that IRF2 modulates the differentiation of haematopoietic cells [24–26]. Despite the unveiling of the molecular pathway of IFN signalling, it remains unclear why IFN-based therapy induces divergent efficacy or adverse haematologic toxicities in different patients.

In the present study, therefore, in order to determine the genetic factors associated with not only the efficacy but also haematologic toxicity of IFN-based therapy, we focused on the genes involved in the IFN signalling pathway, and performed a large-scale and comprehensive analysis of the genetic polymorphisms in 12 genes among chronic hepatitis C patients receiving IFN plus RBV therapy. To identify the predictors of efficacy or haematologic toxicity of IFN-based therapy, we carried out multivariate analyses using various clinicopathological factors and genetic polymorphisms.

MATERIALS AND METHODS

Patients

DNA for SNP screening was extracted from blood samples of 32 healthy Japanese volunteers under the auspices of the Pharma SNP Consortium (Tokyo, Japan). The participants comprised 240 Japanese adult chronic hepatitis C patients receiving conventional IFN-α 2b (n = 157) or peg-IFN-α 2b (n = 83) plus RBV combination therapy (Schering-Plough, Kenilworth, NJ, USA) at Kyoto University and affiliated hospitals from February 2002 to August 2007. In Japan, peg-IFN-α 2b plus RBV combination therapy was approved in October 2004. Thus, the patients who participated before and after October 2004 received conventional IFN-α 2b and peg-IFN-α 2b, respectively. Indications for IFN-based therapy included high serum values of alanine aminotransferase (ALT) and positivity for serum anti-HCV and HCV RNA. Histological examination of liver biopsy specimens was avail able for 165 (68.8%) of the 240 enrolled patients. Liver histology was assessed by an experienced hepatopathologist using the METAVIR score [27]; the fibrosis stage was defined as: F0 (no fibrosis), F1 (mild fibrosis), F2 (moderate fibrosis), F3 (severe fibrosis) and F4 (cirrhosis). The ethics committee at Kyoto University approved the studies, and informed consent for participation in the study was obtained from all patients.

IFN-α 2b or peg-IFN-α 2b plus RBV combination therapy

Patients receiving conventional IFN-α plus RBV therapy were treated with 6 million units of recombinant IFN-α 2b daily for 2 weeks and with 6 million units three times a week for the following assigned treatment period, in combination with daily oral RBV. The RBV dose was 600 mg/day in patients weighing less than 60 kg, and 800 mg/day in those weighing 60 kg or more. Patients receiving peg-IFN-α 2b plus RBV therapy were treated with peg-IFN-α 2b once per week, combined with daily oral RBV for the assigned period. The peg-IFN-α 2b dose was 1.5 μg/kg per week. Patients with genotype 1 received 48 weeks of combination therapy and patients with genotypes 2 and 3 received 24 weeks of combination therapy.

The dosage of IFN-α 2b or peg-IFN-α 2b was reduced by half if platelet counts dropped to <80 000/μL, if leucocyte counts dropped to <1500/μL, or if neutrophil counts dropped to <750/μL during therapy. IFN-α 2b or peg-IFN-α 2b was discontinued if platelet counts dropped to <50 000/μL, if leucocyte counts dropped to <1000/μL, or if neutrophil counts dropped to <500/μL during therapy. The RBV dosage was reduced to 400 mg/day or 600 mg/day if haemoglobin levels were less than 10 g/dL. RBV was discontinued if haemoglobin levels were less than 8.5 g/dL.

Sustained virologic response was defined as no detectable HCV RNA by qualitative assay for at least 24 weeks after cessation of therapy. Non-SVR was defined as no response or relapse after the cessation of therapy.

SNP screening of the IFN signalling pathway-related genes

We selected the following IFN signalling pathway-related genes, including seven genes involved in the intracellular IFN-mediated signalling pathway from the binding of IFN to its receptor to initiation of the transcription of various target genes [20]; four genes involved in the RIG-I signalling pathway, which triggers the IFN-induction pathway after viral infection [22,23], and one gene that negatively regulates the IFN signalling pathway [24] [IFNAR1 (NT_011512.10, NM_000629.2), IFNAR2 (NT_011512.10, NM_207585.1), JAK1 (NT_032977.7, NM_002227.1), TYK2 (NT_011295.10, NM_003331.3), STAT1 (NT_005403.15, NM_007315.2), STAT2 (NT_029419.10, NM_005419.2), IRF9 (NT_026437.11, NM_006084.3), RIG-I (NT_

008413.16, NM_014314.2), IPS-1 (NT_011387.8, NM_020746.1), IRF3 (NT_011109.15, NM_001571.2), IRF7 (NT_035113.6, NM_004031.1), and IRF2 (NT_0022792.17, NM_002199.3)]. Genomic DNA was extracted from blood samples of 32 healthy Japanese volunteers using a DNA extraction kit (Genomix Kit; TALENT, Trieste, Italy), and the 179 exons, including the 5′- and 3′-untranslated regions and adjacent intronic regions of the 12 candidate genes, were amplified. The resultant polymerase chain reaction (PCR) products were used as templates for direct sequencing on an ABI 3730 automated sequencer (Applied Biosystems, Foster City, CA, USA). Segregating sites were identified and genotypes were confirmed directly from electrophorograms using Genalys (http://www.software.cng.fr/docs/genalys.html) [28].

SNP genotyping

Among the SNPs identified by the screening, we selected tag SNP markers that covered all of the common (>5% frequency) haplotypes using the minimal haplotype tagging method, one of the best methods to identify the smallest tagging set for an arbitrary region of the genome [29]. These tag SNPs allowed us to genotype the smallest possible number of SNPs for each gene while resolving all common haplotypes. We also included SNPs that existed in coding sequences or 5′ flanking regions with frequencies higher than 5%. These SNPs were genotyped using the ABI Taqman allelic discrimination method and an ABI 7900HT sequence detection system (Applied Biosystems). Primers and probes were designed by the manufacturer with SNP browser Software (Applied Biosystems), as shown in Tables S1 and S2. Amplification reactions were performed in a 3 μL volume, with 5 ng DNA, 1.5 μL universal PCR master-mix, and 0.0375 μL assay mix with the specific primers and probes. Seven SNPs that could not be detected using the Taqman assay were determined by direct sequencing of PCR products amplified with primers specific for each SNP (Table S3).

Statistical analysis

Genotype distributions were tested for Hardy–Weinberg equilibrium using exact tests. To identify predictors of SVR, we used univariate analysis of pre-treatment factors to compare all SVR and non-SVR patients who had completed the treatment. The following pre-treatment factors were considered: SNPs, sex (male *vs* female), age (in years), weight (in kilograms), serum ALT, IFN history (naive *vs* relapse *vs* nonresponse), HCV genotype (1 *vs* 2 and 3), HCV viral load (<100 *vs* 100 to <500 *vs* 500 to <850 *vs* ≥850 kIU/mL), and fibrosis stage (F0 *vs* F1 *vs* F3 *vs* F4). Allele and genotype frequencies were evaluated for their association with SVR using Fisher's exact tests. Sex, IFN history, and HCV genotype were evaluated using the chi-square test. Age, weight, and serum ALT were evaluated using the Mann–Whitney *U*-test. Fibrosis stage and viral load were evaluated using a trend chi-square test. We considered two-tailed *P*-values <0.05 to be statistically significant and calculated odds ratios (ORs) and 95% confidence intervals. Multiple logistic regression analysis was performed using STATISTICA (StatSoft, Tulsa, OK, USA) to evaluate the association between SVR and significant factors from the univariate analyses.

To identify predictors of cytopenia, we examined the association between decreased leucocyte, neutrophil, and platelet counts and haemoglobin levels, and the following patient characteristics and clinical features using linear regression analysis with STATISTICA: sex, age, weight, fibrosis stage and SNPs. Multiple linear regression analysis was performed to evaluate the association between the decreased peripheral blood cell numbers and significant factors from the univariate analyses.

RESULTS

Genetic variations and polymorphisms in IFN signalling pathway-related genes

By screening 32 healthy volunteers, we identified 167 genetic polymorphisms (153 SNPs and 14 insertions/deletions) in the 12 IFN signalling pathway-related genes (Table 1, Table S4). All identified polymorphisms were in Hardy–Weinberg equilibrium. Of these 167 polymorphisms, 60 (49 SNPs and 11 insertions/deletions) were novel and were not registered in Build 125 of the SNP database (http://www.ncbi.nlm.nih.gov) (Table 2). Among the 167 SNPs identified, 30 (16 nonsynonymous and 14 synonymous) were located in exons and we confirmed that 14 of the 30 SNPs identified in the exons were novel. Furthermore, we identified 10 novel nonsynonymous variants in the seven genes. Sixty-two SNPs were relatively uncommon (minor allele frequency <0.05) and were thus excluded from further analysis. Finally, 27 selected tag SNPs and eight additional SNPs that existed in coding sequences or 5′ flanking regions were subjected to further genotyping analyses in chronic hepatitis C patients (Table 2).

Variables associated with virologic response to IFN-based therapy

The relationship between baseline characteristics and virologic response to the IFN plus RBV combination therapy in chronic hepatitis C patients is summarized in Table 3. Combination therapy was discontinued in 37 patients during the assigned treatment period. These 37 patients were excluded from analysis of the virologic response. SVR was achieved in 98 of 203 (48.3%) patients, and 105 patients (51.7%) had a relapse of HCV infection after the end of therapy or showed no response to IFN-based therapy.

To determine the predictive factors for IFN-based therapy efficacy, we examined the correlation between virologic response, and clinical and viral factors. Of 56 patients with